



www.bioinformation.net
Volume 18(10)

Research Article

Received September 2, 2022; Revised October 3, 2022; Accepted October 6, 2022, Published October 31, 2022

DOI: 10.6026/97320630018870

Declaration on Publication Ethics:

The author's state that they adhere with COPE guidelines on publishing ethics as described elsewhere at <https://publicationethics.org/>. The authors also undertake that they are not associated with any other third party (governmental or non-governmental agencies) linking with any form of unethical issues connecting to this publication. The authors also declare that they are not withholding any information that is misleading to the publisher in regard to this article.

Declaration on official E-mail:

The corresponding author declares that lifetime official e-mail from their institution is not available for all authors

License statement:

This is an Open Access article which permits unrestricted use, distribution, and reproduction in any medium, provided the original work is properly credited. This is distributed under the terms of the Creative Commons Attribution License

Comments from readers:

Articles published in BIOINFORMATION are open for relevant post publication comments and criticisms, which will be published immediately linking to the original article without open access charges. Comments should be concise, coherent and critical in less than 1000 words.

Edited by P Kanguane

Citation: Prabhu *et al.* Bioinformation 18(10): 870-875 (2022)

Anti-cancer activity of *C. cainito* leaves explained using its compounds docked with p53

Yesudass Antony Prabhu¹, Chinnasamy Balalakshmi², Muthu Vijayasarathy³, Kumar Praveen Kumar⁴, Piramanayagam Shanmughavel⁵ & Samiappan Kavitha^{6*}

¹Department of Biochemistry, Rathnavel Subramaniam College of Arts and Science, Bharathiar University, Coimbatore - 641402, India; ²Department of Nanoscience and Technology, Alagappa University, Karaikudi - 630003, India; ³Department of Microbiology, Thiagarajar College of Arts and Science, Madurai, India; ⁴Department of Bioinformatics, Bharathiar University, Coimbatore - 641046, India; ⁵Department of Bioinformatics, Bharathiar University, Coimbatore - 641046, India; ⁶Department of Biochemistry, Rathnavel Subramaniam College of Arts and Science, Bharathiar University, Coimbatore - 641402, India; *Corresponding author: Samiappan Kavitha: kavithabiochemist@yahoo.com & skavitha@rvsgroup.com

Author contacts:

Yesudass Antony Prabhu - E-mail: antonybiochemist@gmail.com, <https://www.rvscas.ac.in/> & <https://b-u.ac.in/>

Chinnasamy Balalakshmi - E-mail: samyasribala@gmail.com, <https://www.alagappauniversity.ac.in/>

Muthu Vijayasarathy - E-mail: vijayasathymvs@gmail.com, <https://www.tcarts.in/>

Kumar Praveen Kumar - E-mail: sirajane@gmail.com, <https://b-u.ac.in/>

Piramanayagam Shanmughavel - E-mail: shanmughavel@buc.edu.in; <https://b-u.ac.in/>

Samiappan Kavitha - E-mail: kavithabiochemist@yahoo.com & skavitha@rvsgroup.com, <https://www.rvscas.ac.in/>

Abstract:

Extensive research on the mutant P53 protein has identified its pivotal role in anti-apoptosis mechanisms, drug resistance, and cancer progression in OSCC. The mass spectrum revealed the pharmacologically significant bioactive compounds reported for the first time in *C. cainito*. Molecular docking investigation has identified four potential new P53 inhibitors compared with the standard P53 inhibitors. Hence, this analysis reinforces the likelihood of anti-cancer activities in *C. cainito* leaves.

Keywords: molecular docking, mutant P53 inhibitors, *C. cainito*, and OSCC

Background:

OSCC is a heterogeneous group of cancers in the oral cavity, accounting for about 90% of all oral malignancies [1-2]. The traditional risk factors associated with OSCC include smoking habits with a cigarette, bidis, kretek or water pipe; chewing habits with betel squid, pan masala, and consumption of excessive alcohol [3]. Most significantly, the habits of tobacco smoking and alcohol consumption potentiate the induction of p53 mutations in nearly 65-85% of OSCC patients [4]. Generally, wild-type p53 mediates cell cycle arrest by p21 activation, regulation of DNA repair, and apoptosis induction which acts as a tumor suppressor gene and prevents OSCC progression. Conversely, a mutation in p53 leads to the gain of proto-oncogenic function, thereby increasing the progression of tumorigenesis and carcinogenesis. Thus, p53 mutants have become a popular target for developing new cancer therapeutics [5]. Furthermore, patients who underwent cancer therapy, such as chemotherapy and radiation therapy, have developed drug resistance, promoting tumor progression, and poor survival, and are associated with the p53 mutation [6]. Recent research has uncovered that alteration of the p53-encoding gene TP53 is the most direct and effective route to inactivate p53 [7]. Consequently, it is difficult to cure cancer, and the incidence of OSCC has expected to be more in the future in India [2]. Intrinsically, such mutations interfere with anti-apoptotic mechanisms in the OSCC. Hence, it is of interest to document the effective anti-mutant p53 inhibitors from *C. cainito* leaves using molecular docking.

Materials and methods:**Plant collection:**

The fresh and healthy leaves of *C. cainito* (latitude 11.01° N, longitude: 76.9 5° E) were collected with fruit specimens and submitted for authenticity at the Botanical Survey of India, Tamilnadu Agricultural University campus, Coimbatore. Subsequently, we received for voucher number of the analyzed specimen as BSI/SRC/5/23/2020/Tech/808.

Soxhlet extraction of plant material:

At the onset, *C. cainito* leaves were washed three times with ultra-pure Milli Q water to clean off impurities and soil. After drying them at room temperature for a week, it was well pulverized and stored in an airtight jar until needed. For soxhlet extraction, 100 grams of *C. cainito* leaves powder were subjected to ethanolic extractions using the soxhlet apparatus at 60°C for 12 hours. In this extraction, HPLC grade of solvent was used. Subsequently, the concentrated ethanolic sample was kept at 50°C for two days in a hot air oven on a washed petri plate and analyzed using GCMS.

Phytochemical analysis using GC-MS:

The bioactive compounds presence in the ethanolic extract of the *C. cainito* specimen had explored by Thermo MS DSQ II, Thermo Fisher Scientific, United States. For a sample running GCMS conditions, refer to our journal [2]. The analyzed chromatogram of ethanolic extract of *C. cainito* is shown in Figure 1.

Molecular Docking:

Molecular docking analysis approach was performed using the maestro module of the Schrodinger suite because of its intuitive molecular modelling environment-like features for medicament discovery. The Glide module of the XP visualizer was used with the OPLS-2005 force field to identify an interaction between *C. cainito* ligands and altered p53 protein binding sites, as well as their affinity [2].

Preparation of protein:

The 3-dimensional molecular structure of a mutant P53 protein (6GGE) is obtained from PDB website (website link: <https://www.rcsb.org/>). The 6GGE protein was prepared using the protein preparation wizard tool (prep wizard) in Schrodinger Suite, 2018. Prep wizard is an indispensable tool for researchers to correct the structural imperfections [8-9]. Figure 2 illustrates the massive disparities between unprocessed and preprocessed 6GGE structures. The unprocessed structure of 6GGE was found to hold faults, whereas the preprocessed protein structure is subjected to a prep wizard. All 3D structures of *C. cainito* phytonutrients were retrieved from the PubChem database and created as ligands using the Lig Prep module in the same Schrodinger suite using GCMS results [10]. However, the computational investigations require the following features like default parameters: 3D structures conversion, precise lewis chemistry, stereoisomers, ring conformations, limits the computational errors, and customizable libraries. Phytonutrients analyzed from an ethanolic extract of *C. cainito* are listed in Table 1 and whereas Figure 3 illustrates the structures of all the investigated chemical compounds.

Analysis of ADME/T property:

Several medicaments failed nearly 40% in clinical trials due to poor ADME characteristics. Late-stage failures are a major contributor to the rising expense of new therapeutic development. The QikProp tool predicts the properties of molecules with new scaffolds and analogs of well-known medications with comparable accuracy. By which, the ADME/T characteristics of the best four interacted ligands over 6GGE were assessed using the QikProp module in the Schrodinger suite. QikProp investigation exposed significant physicochemical characteristics and pharmacokinetic relevant features (Table 2) [2].

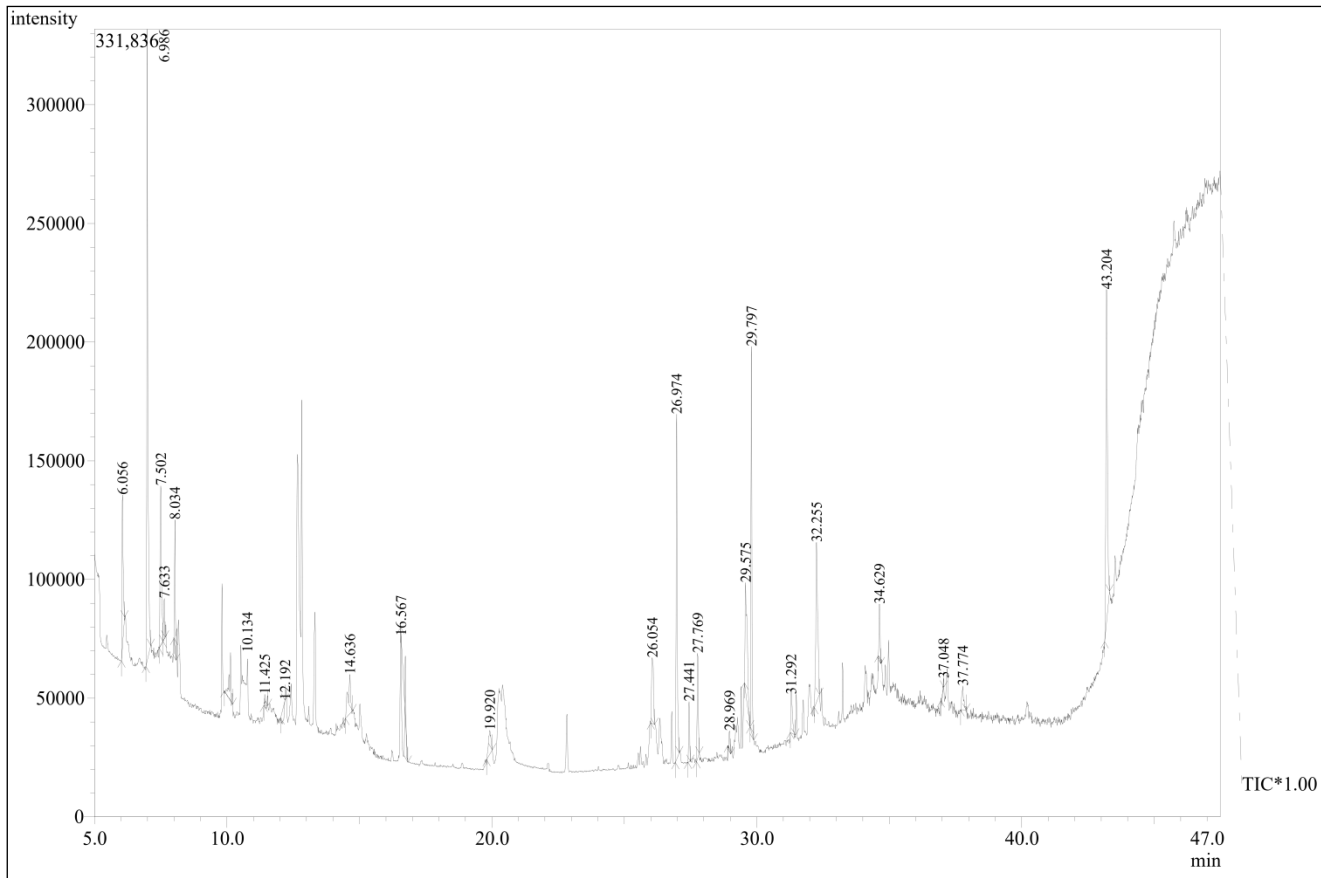


Figure 1: GC-MS chromatogram of ethanolic extract of *C. cainito* leaves

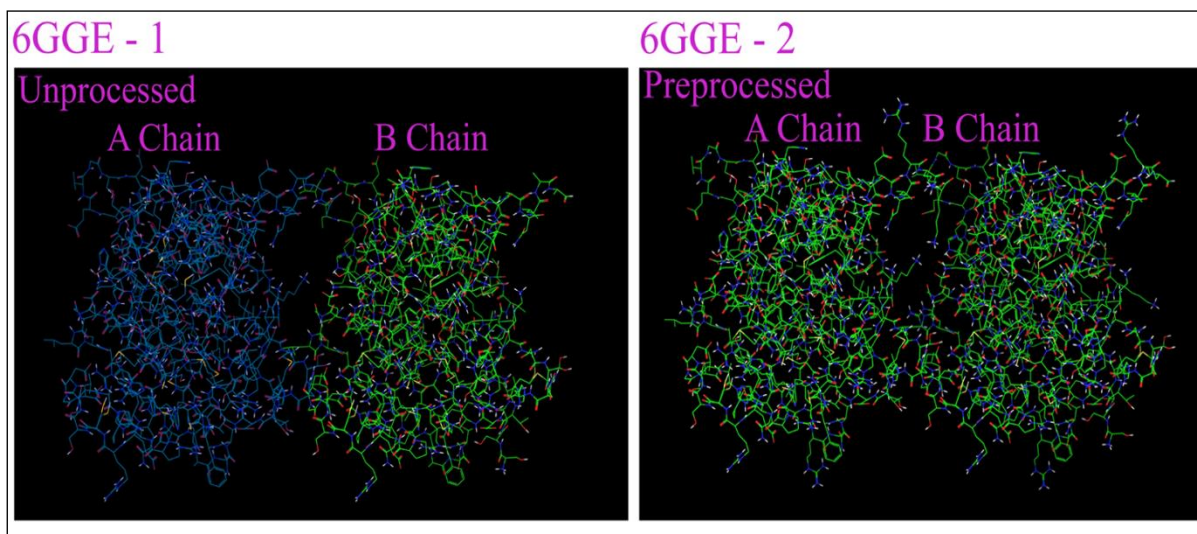


Figure 2: 3D Structure of the mutant P53 protein A and B chains (PDB ID: 6GGE). The unprocessed A chain (colored in blue) and B chain (colored in green) in the 6GGE-1 picture both contain faults in their structure (before prep wizard). But 6GGE-2 preprocessed A and B chains that do not have defects developed by the prep wizard.

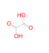

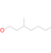
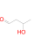




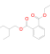
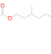
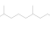

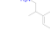










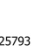

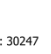
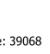
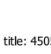
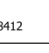
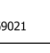
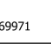

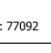

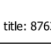
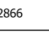
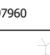
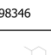
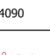
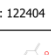
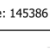
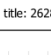
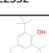


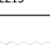

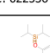
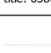
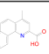
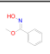
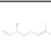



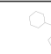
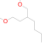

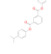




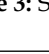
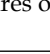
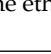
 title: 971	 title: 6517	 title: 7792	 title: 7897	 title: 8193	 title: 8195	 title: 8217
 title: 8221	 title: 8343	 title: 8834	 title: 10446	 title: 10472	 title: 11398	 title: 12395
 title: 12397	 title: 12404	 title: 12542	 title: 12620	 title: 15076	 title: 17697	 title: 18693
 title: 21584	 title: 23701	 title: 25793	 title: 29075	 title: 30247	 title: 39068	 title: 45056
 title: 68412	 title: 69021	 title: 69971	 title: 74822	 title: 77092	 title: 79299	 title: 87635
 title: 92866	 title: 97960	 title: 98346	 title: 104090	 title: 122404	 title: 145386	 title: 262858
 title: 522532	 title: 545786	 title: 549909	 title: 552215	 title: 585001	 title: 622536	 title: 638072
 title: 3960962	 title: 5280435	 title: 5364982	 title: 5365037	 title: 5366013	 title: 6327720	 title: 6327799
 title: 6425096	 title: 9602988	 title: 10997105	 title: 12656862	 title: 13656289	 title: 14168667	 title: 54979384
 title: 91692255	 title: 91695521	 title: 91739884				

Figure 3: Structures of all the ethanolic *C cainito* bioactive compounds as determined by the GCMS library, along with their PubChem IDs

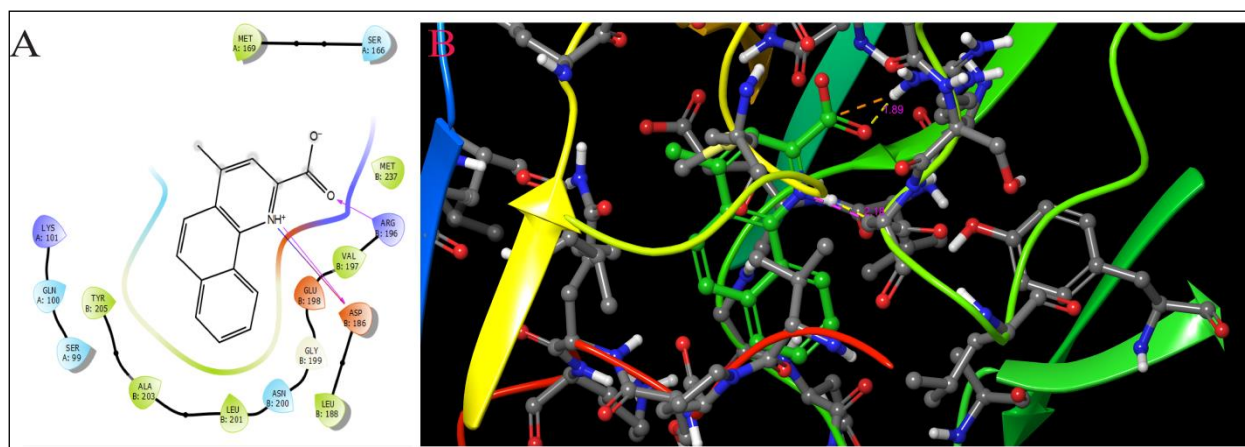


Figure 4: shows the most potent mutant p53 inhibitor from *C cainito*, MACA, interacted with a mutant P53 molecule in virtual screening. A) The 2-dimensional structure of MACA and its interaction with p53, with arrows showing the specific binding site; B) Depicts the same molecule's three-dimensional structure in great detail.

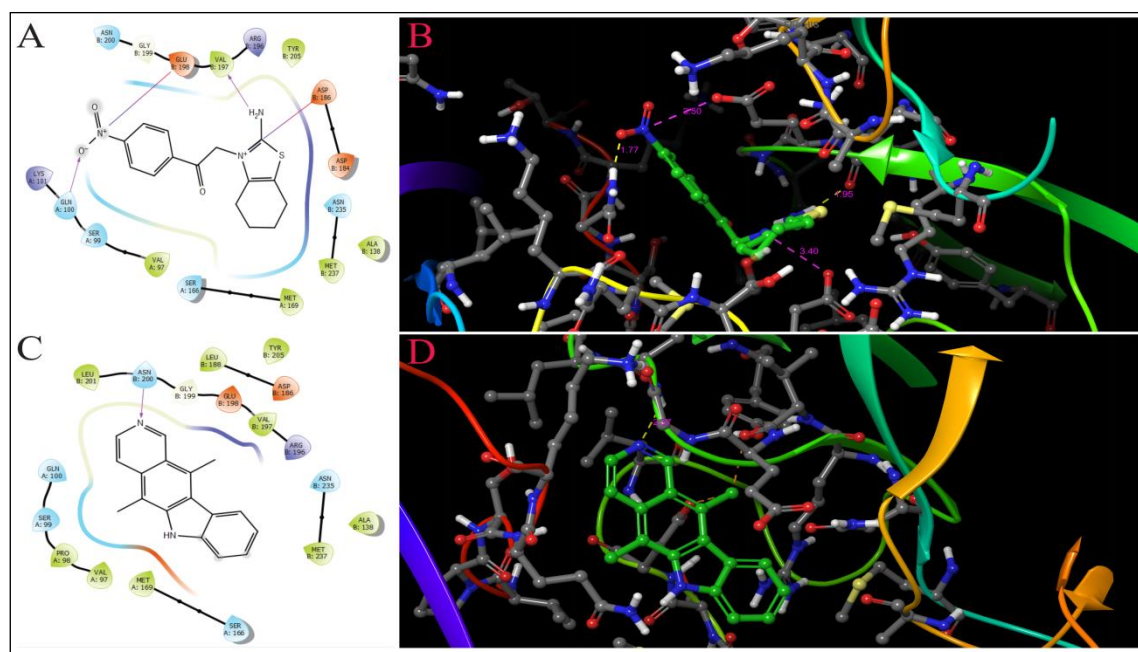


Figure 5: shows the interaction of the standard P53 drugs such as pifithrin- α p-nitro and ellipticine. A) Shows the interaction of pifithrin- α p-nitro ligand on the residue of mutant p53 and B) illustrates the same structure in 3D with a ribbon-like representations view. C) Exhibits the binding of ellipticine 2D structure on a mutant P53 receptor amino acid residue D) displays the same interaction in a 3D view.

Table 1: Summarizes the structure of the GCMS examined ethanolic extract of *C. canito* (whereas, figure 3 shows the structure of all the library compounds with pub chem ID)

Peak	R. Time	I. Time	F. time	Area	Area %	Height	Height %	A/H	Mark
1	6.056	6.017	6.133	182596	4.66	63740	5.15	2.86	
2	6.986	6.942	7.125	754415	19.26	266249	21.52	2.83	
3	7.502	7.442	7.583	256440	6.55	67164	5.43	3.82	
4	7.633	7.583	7.667	40413	1.03	16909	1.37	2.39	V
5	8.034	8	8.075	109580	2.8	54081	4.37	2.03	
6	10.134	9.9	10.217	78997	2.02	20325	1.64	3.9	MI
7	11.425	11.392	11.55	9755	0.25	4549	0.37	2.14	MI
8	12.192	12.025	12.192	-33914	-0.87	0	0	-181.59	MI
9	14.636	14.475	14.742	107980	2.76	16507	1.33	6.51	MI
10	16.567	16.558	16.825	-205380	-5.24	-1917	-0.15	-8.42	MI
11	19.92	19.8	20.017	65186	1.66	10041	0.81	6.4	MI
12	26.054	26	26.142	135780	3.47	27641	2.23	4.91	
13	26.974	26.925	27.075	441404	11.27	145418	11.75	3.04	
14	27.441	27.4	27.492	69012	1.76	25373	2.05	2.72	
15	27.769	27.725	27.833	130245	3.33	44214	3.57	2.95	
16	28.969	28.908	29.017	20733	0.53	8122	0.66	2.61	MI
17	29.575	29.533	29.75	257690	6.58	45771	3.7	5.63	
18	29.797	29.75	29.883	415355	10.61	162146	13.11	2.56	
19	31.292	31.267	31.458	68971	1.76	16158	1.31	4.27	
20	32.255	32.175	32.367	330700	8.44	67302	5.44	4.91	
21	34.629	34.592	34.683	64826	1.66	23080	1.87	2.81	
22	37.048	36.95	37.058	2516	0.06	4109	0.33	0.6	MI
23	37.774	37.692	37.908	45121	1.15	10019	0.81	4.5	MI
24	43.204	43.133	43.317	568167	14.51	140076	11.32	4.06	

Table 2: Lists the ADMET characteristics of bioactive compounds found in the ethanolic extract of *C. canito*

S. no	Bioactive compounds	Mol-MW	Donor		Accept		Human oral absorption	% Human oral absorption
			HB	HB	HB	HB		
1	1-Methyl-4-azaphenanthrene-3- carboxylic acid	237.257	1	3			3	85.994
2	2-Hydroxyacetamide	75.067	3	4.2			2	50.563
3	2-Phenylprophylamine	135.208	2	1			3	88.226
4	Dihydroxymalonic acid	136.061	2	3.5			1	27.428

Table 3: Energy data for ethanolic *C. canito* ligands which interacted with P53 are listed

S. no	Bioactive compounds	GScore	DScore	HBond
1	1-Methyl-4-azaphenanthrene-3- carboxylic acid	-6.08	-4.03	-1.72
2	2-hydroxyacetamide	-4.63	-4.63	-2.97
3	2-Phenylprophylamine	-4.45	-4.45	-0.11
4	Dihydroxymalonic acid	-4.29	-4.29	-2.44

5	Pifithrin- α p-nitro (P53 standard inhibitor, Pub chem ID: 11553038)	-3.81	-3.8	-0.7
6	Ellipticine (P53 standard inhibitor, Pub chem ID: 3213)	-3.76	-1.68	-0.53

Table 4: Lists the residue data for the best four *C. cainito* ligands that have interacted with P53

S. no	Bioactive compounds	Interacting residues	Bond length
1	1-Methyl-4-azaphenanthrene-3- carboxylic acid	ASP 186, ARG 196	2.18 Å, 2.42 Å, and 1.89 Å
2	2-hydroxyacetamide	ASN 200, GLY199, VAL 197 and ASP186	1.91 Å, 2.08 Å, 1.98 and 1.79
3	2-Phenylprophylamine	VAL 197 and ASP 186	2.58 and 2.73
4	Dihydroxymalonic acid	GLN 100, SER 99, ASN 200 and GLY 199	1.90, 2.07, 1.97 and 2.57

Results and Discussion:

It is the first investigation which is performed from ethanolic extract of *C cainito* leaves against mutant P53. Thereof, MACA interacts with 6GGE molecules as shown in Figure 4 A and B. Ligand formed a strong hydrogen bond with the mutant p53 receptor amino acid residues at arginine 196 and asparagine 186 during this interaction. These molecules have bond distances of 2.18, 2.42, and 1.89, respectively. The top four ligands that interacted with the mutant P53 receptor (as indicated in Table 3) had docking GS scores of -6.08, -4.63, -4.45, and -4.29, respectively. These ligands include MACA, 2-hydroxyacetamide, 2-phenylprophylamine, and dihydroxymalonic acid. A greater negative GScore has a better interaction [11] and Table 3 also lists other metrics such as dock score and H bond. Table 4, the ligand-interacting amino acid residues and bond lengths of the molecules are listed. This study uncovered a unique MACA interaction that is expected to have the same function and anti-cancer properties. For instance, molecular docking research by Hussan and colleagues [12] showed that benzalkonium ibuprofenate interacted better than built-in standard ligands with a receptor. In a similar fashion, we have sought to validate such feasibility with a commonly known two standard p53 inhibitors, such as ellipticine and pifithrin- α p-nitro [13-14]. Surprisingly, we found that our four ligands are mentioned above interacted more strongly with mutant p53 than the standard p53. The pifithrin- α p-nitro had interacted slightly effectively as compared with ellipticine, at the docking scores of -3.81 and -3.76. This evidence reinforces the *in-silico* approach and the prospect of finding novel mutant p53 inhibitors from the medicinal plant *C cainito* (Figure 5 and Table 3). Next to that MACA inhibitor, the other three ligand interactions at binding sites, bond type, and length, as well as providing GScore, are shown in Figure 5. Furthermore, ADMET characteristics of bioactive compounds discovered in the ethanolic extract of *C cainito* are reported in Table 2 MACA and 2-phenylprophylamine have good properties.

Conclusion:

Data reports the potent four effective mutant P53 inhibitors from the *C cainito* leaves, which hold better binding properties than ellipticine and pifithrin- α p-nitro. With the highest docking score over the mutant P53 receptor as compared to 2-hydroxyacetamide, 2-phenylprophylamine, and dihydroxymalonic acid, MACA

inhibitors are the best ligands for interactions. However, further analysis of ADME/T characteristics demonstrated the drug-likeness for 2-phenylprophylamine and MACA bioactive compounds. On the other side, 2-hydroxyacetamide and dihydroxymalonic acid had minimal pharmacokinetic properties. Therefore, we suggest that MACA and 2-phenylprophylamine are novel mutant P53 inhibitors that deserve augmented attention as anti-cancer agents.

Acknowledgement

The DBT-Centre for Bioinformatics at Bharathiar University in Coimbatore, Tamil Nadu, India, is appreciated for kindly offering all the materials required to finish this project.

Conflicts of interest

The authors claim that they do not have any conflicts of interest.

References:

- [1] Chai AWY *et al. Semin Cancer Biol.* 2020 **61**:71. [PMID: 31542510]
- [2] Prabhu YA *et al. Bioinformation.* 2021 **17**:550. [PMID: 35095229]
- [3] Bugshan A & Farooq I, *F1000Res.* 2020 **9**:229. [PMID: 32399208]
- [4] Lindemann A *et al. J Dent Res.* 2018 **97**:635. [PMID: 29489434]
- [5] Giacomelli AO *et al. Nature genetics.* 2018. **50**:1381. [PMID: 30224644]
- [6] Ahmadi N *et al. Oral Surg Oral Med Oral Pathol Oral Radiol.* 2019 **128**:631. [PMID: 31495715]
- [7] Zhou X *et al. J Mol Cell Biol.* 2019 **11**:293. [PMID: 30508182]
- [8] Negron C *et al. Plos one.* 2019 **14**:e0214015 [PMID: 30889230]
- [9] Prabhu YA *et al. IJPRSE.* 2022 **3**:21.
- [10] Kumar PK & Piramanayagam S, *Bioinformation.* 2021 **17**:369 [PMID: 34092958]
- [11] Acharya R *et al. Scientific reports.* 2019 **9**:15743. [PMID: 31673107]
- [12] <https://www.intechopen.com/chapters/71208>
- [13] Murphy PJ *et al. J Biol Chem.* 2004 **279**:30195. [PMID: 15145929]
- [14] Peng Y *et al. Oncogene.* 2003 **22**:4478. [PMID: 12881704]